Experimental Modal Analysis on a Rotating Fan Using Tracking-CSLDV

Andrea Gasparoni [a], Matthew S. Allen [b], Shifei Yang [b], Michael W. Sracic [b], Paolo Castellini [a] and Enrico P. Tomasini [a]

[a] *Dipartimento di Meccanica, Università Politecnica delle Marche*
Via Brecce Bianche,60131 Ancona, IT
[b] *Department of Engineering Physics, University of Wisconsin-Madison*
535 Engineering Research Building,
1500 Engineering Drive,
Madison, WI 53706, USA

Email: msallen@engr.wisc.edu

Abstract. Continuous Scan Laser Doppler Vibrometry (CSLDV) modifies the traditional mode of operation of a vibrometer by sweeping the laser measurement point continuously over the structure while measuring, enabling one to measure spatially detailed mode shapes quickly and minimizing the inconsistencies that can arise if the structure or test conditions change with time. When a periodic scan path is employed, one can decompose the measurement into the response that would have been measured at each point traversed by the laser and obtain the structure's mode shapes and natural frequencies using conventional modal analysis software. In this paper, continuous-scan vibrometry is performed on a rotating fan, using computer controlled mirrors to track the rotating fan blades while simultaneously sweeping the measurement point over the blades. This has the potential to circumvent the difficulty of attaching contact sensors such as strain gauges, which might modify the structure and invalidate the results. In this work, impact excitation was used to excite a 3-blade fan rotating at various speeds, and the blades were scanned with a cloverleaf pattern that captured the bending of all three blades simultaneously. Some specialized signal processing is helpful in minimizing the effect of rotation frequency harmonics in the measurements, and specific scan strategies are needed to avoid those frequencies, both of these issues are discussed in the paper. While noise in the laser vibrometer does pose some difficulty, the results show that several modes could be extracted and that the tracking-CSLDV results agree with measurements obtained from the parked fan.

Keywords: Vibrations, Doppler, Laser, LDV, Tracking, TLDV, Continuous, CSLDV, Rotating, Modal, ODS.
PACS: 43.40.+s, 06.60.Mr, 07.05.Kf, 07.60.Ly, 43.40.Yq

1. INTRODUCTION

In recent years Laser Doppler Vibrometry has proven to be a very powerful technique for characterizing vibrating structures. Not only does it allow for highly sensitive, non-intrusive measurements, but the LDV can also be coupled to a simple pair of scanning mirrors (usually driven by galvanometer motors), allowing the measurement point to be changed quickly and easily, unleashing the imagination of the researcher to pursue dramatically new approaches to taking measurements, processing data and extracting information. New concepts have been explored to extend measurement capabilities and to reduce the time and effort required for experimental tests.

Using the conventional SLDV approach, the measurements must be repeated at each point on the structure to obtain the mode shapes of the structure. This point by point approach may be inaccurate if properties of the structure change with time, temperature or other environmental parameters, or if one wishes to use inputs that are difficult to replicate, such as blast or impact loads. Also it may take quite a long time to acquire measurements at many points on a structure if those points must be acquired one at a time, particularly if the structure has lightly damped, low frequency modes. In light of these limitations, some researchers have suggested sweeping the laser spot continuously

over the structure while measuring its response to try to measure the structure's mode shapes and natural frequencies simultaneously.

The first concept developed was the Continuous Scanning CSLD [1, 2] where the laser beam was moved during the measurement in order to extract ODS more quickly, directly acquiring a polynomial representation of the mode shape and finally to reconstruct the shape at many points on the structure.

In the same period the Tracking LDV concept [3-5] was developed and studied by other authors. Usually structural characterization of rotating objects is performed by modal analysis in static condition by Impact Testing. But it is very important to join an improved structural model of the structure under analysis and its aerodynamic model to study aero-elastic behavior. The galvo movement was there used to track the movement of the target, both in rotating or in a-priori unknown trajectories. So the TLDV, measuring the response of a structure as it moves, allows structural characterization of rotating objects in operational conditions. Most subsequent works have been concerned with rotating targets, which represent one of the most common needs.

More recently the two concepts were combined, developing the tracking version of the CSLDV [6]. Other authors developed an alternative way to process the CSLDV data and extract information [7], which reduces the effort required to extract the modal parameters from the measurements. In this paper this new CSLDV approach was extended to the 2D scanning on a rotating fan. The configuration studied is representative of many bladed structures, so the approach should be straightforward to generalize to other systems such as helicopter blades, turbo machinery etc…

The rest of the paper is organized as follows. Section 2.1 briefly reviews the CSLDV approach used in this work, while Section 2.2 discusses the modifications that were needed to use this while tracking a rotating structure. Section 3 discusses the experimental setup and the results that were obtained using this approach to test a parked fan in Section 3.1 and a rotating fan in 3.2. The conclusions are presented in Section 4.

2. THEORY

This section briefly reviews the CSLDV approach used in this work, which is described in detail in [7,8], and discusses the modifications that were necessary to acquire and process continuous-scan LDV measurements while tracking a rotating structure.

2.1. Review of CSLDV Approach

The approach used in this work utilizes only the free response of the vibrating structure, which can be written in the following state space form for an arbitrarily damped linear system with N underdamped modes

$$y(t)=\sum_{r=1}^{2N}\phi_r(\mathbf{x})C_r e^{\lambda_r t}$$

$$\left.\begin{aligned}\lambda_r &= -\zeta_r\omega_r + i\omega_r\sqrt{1-\zeta_r^{\,2}}\\ \lambda_{r+N} &= \lambda_r^{\,*}\end{aligned}\right\} r=1\ldots N \tag{1}$$

where λ_r is the rth complex eigenvalue, which is expressed in terms of the rth natural frequency, ω_r, and damping ratio, ζ_r. The complex constant C_r is the complex amplitude of mode r. It depends on the structure's initial conditions and hence on the impulse used to excite the structure. The response of such a system can be measured at a point that changes with time using the experimental setup described in Section 3. In this work the motion of the laser measurement point is limited to a three-dimensional periodic path, $x(t)= x(t+T_A)$, whose period is T_A. The fundamental frequency of the scan pattern is then $\omega_A=2\pi/T_A$. Since the scan pattern is periodic, the mode vector becomes a periodic function of time, and the response can be written as

$$\begin{aligned}y(t)&=\sum_{r=1}^{2N}\phi_r(t)C_r e^{\lambda_r t}\\ \phi_r(t)&=\phi_r(t+T_A)\end{aligned} \tag{2}$$

The free response of each mode in the system is a damped harmonic, captured mathematically by the complex exponential $e^{\lambda_r t}$. That (damped) harmonic function is multiplied by the periodic mode vector $\phi_r(t)$. One can

expand $\phi_r(t)$ in a Fourier series and use trig identities to show that each mode manifests itself at a multitude of harmonics, $\omega_r\sqrt{1-\zeta_r^2}+k\omega_A$, where k is a positive or negative integer. The relative amplitudes of the harmonics can be used to determine $\phi_r(t)$ and hence $\phi_r(x)$; this is essentially the basis for one of the methods used by Stanbridge, Martarelli, Ewins, Di Maio and their associates [2,9,10], a variant of which was called the Fourier Series Expansion method in [7,11].

This work focuses on a different approach, which is referred to as lifting in [7,11]. First, the response of the structure is resampled such that there are an integer number of samples per period, T_A. The number of samples per period is denoted N_A. A series of lifted responses are then created, with the k^{th} given by

$$y^*_k = y\left(k\Delta t + mT_A\right) \tag{3}$$

where m is an integer that ranges over the length of the measurement. Since T_A is typically larger than the period of the highest frequency mode in the system, this aliases each of the modes of the system to the frequency band $[0,\omega_A/2]$. Using this procedure, one can create N_A lifted measurements ($k = 1\ldots N_A$), each of which has the same (aliased) natural frequencies since $\phi_r(t)$ is constant in each of the lifted responses. The collection of lifted responses can be used to identify the aliased natural frequencies and damping ratios of the system. The authors have accomplished this by treating the lifted measurements as a single-input-multi-output set of measurements and processing them with a global modal parameter identification routine [12]. The residue vectors of the lifted system are found in this process and the algorithm in [7] is used to extract the time-varying mode shapes $\phi_r(t)$ from them. When the system is lightly damped so that its modes are predominantly real, then the procedure described in [7] can be used to determine the true, unaliased natural frequencies and damping ratios from the identified ones.

2.2. Modifications for T-CSLDV

In this work we seek to apply CSLDV to a rotating object, combining CSLDV with Tracking vibrometry (TLDV). The Tracking Laser Doppler Vibrometry (TLDV) first presented by [4] is a technique based on the use of the Scanning Laser Doppler Vibrometer (SLDV) for Lagrangian measurements. The goal is to lock the laser beam to a single point as that point moves and vibrates with the structure. This enables structural vibrations to be measured in operating conditions. The TLDV is basically a SLDV system modified into a controlled tracking system for rotational motions by driving the two moving mirrors via clock signals generated by an angular position transducer (encoder) linked to the shaft of the rotating device.

The measurements system consists of a vibrometer and a PC. The mirrors of the scanning vibrometer (usually used to move the laser to fixed points on a measurement grid) are driven by a sine and cosine signal respectively: this causes the laser to trace a circle on the surface of projection. The signal generation clock is controlled by the pulse-train signal from an incremental encoder, which measures the instantaneous angular position of the shaft. The control system is based in a PC, which contains a board to generate signals to drive the scanning mirrors and to acquire the measurements of interest.

The tracking LDV requires two galvanometer scanners, one oriented on an *X*-axis and the other on the *Y*-axis. One galvanometer scanner moves the beam horizontally; the other one moves it vertically. This arrangement means the scanners can position the beam anywhere within a square area simply by applying a voltage. The input signal is sent to the scanner drive stage circuit after passing through the input conditioning circuit that converts voltage in current. So supplying voltages V_x and V_y to the scanner drivers causes an angular deflection of each mirror, θ_x and θ_y. Denoting the static sensitivity of the whole galvanometric motor and of the driver system as S_x and S_y, the angles are given by:

$$\begin{aligned}\theta_x &= S_x V_x \\ \theta_y &= S_y V_y\end{aligned} \tag{4}$$

The scanner used is a closed loop type. Each mirror is fitted with a position detector that measures the position of the scanner within its range of motion. This allows the very precise and accurate control of the mirror that is necessary. In this work, those position signals were acquired to determine the scan pattern that was realized and to measure the rotational velocity for the lifting method. Naturally, since this is a mechanical system, there are limits to how fast the mirror can be moved.

Great care was taken to select appropriate components to drive the mirrors and to acquire signals, because tracking requires good timing and synchronization. The data acquisition system selected is a PXI by National

Instruments, which is modular, configurable with a range of boards and allows advanced timing and synchronization. It is also easily programmable with the LabVIEW programming language by the same manufacturer.

The board used to control the mirrors was a NI-PXI-6733 +BNC-2120 connector block. It contains two high speed (20MHz) and high resolution (24 bits) counters. Two counters are needed for tracking, one to acquire encoder 0/rev signal to use as a trigger and know the absolute position of the blade, the other one to acquire the channel A of the encoder that works as clock to move mirror at the same velocity of the blades. When the system rotates at the maximum rotational speed of ~1000 RPM, the 2048 tick encoder signal switches at 34kHz. The bandwidth of the counters is 50 times higher than this, assuring that the ticks will be accurately recorded. Also the 16 bits output resolution of the card allows precise control of mirrors at up to 1 MS/s, which is several orders of magnitude higher than required.

The board used to acquire signals was a NI-PXI-4472 with 8 analog input channels with 24-bit resolution ADCs that are simultaneously sampled over a bandwidth from DC to 45 kHz, software programmable. The 24 bits architecture deliver more than 110 dB dynamic range and since these ADCs use a 1-bit quantizer oversampled at a multiple of the specified sampling rate, they produce good linearity. Also the synchronization between channels allows the resampling process, used to obtain lifted responses, to be free of any delay due to acquisition.

3. EXPERIMENTAL RESULTS

The system studied in this work is shown in FIGURE 1. The structure of interest is a 762mm diameter air conditioning condenser fan, which is mounted in a commercial support structure and powered by a 2 kW, 230V, three-phase motor with a nominal rotational speed of 1140 RPM. In this work, that motor is driven by a variable frequency drive, which allows the speed of the motor to be controlled within certain limits. The motor support structure is mounted in a commercial shroud. This assembly would typically be mounted with the motor axis pointing vertically and several of these units would be installed in parallel in a rigid frame and would operate in unison to pull air past a large chilled-water heat exchanger. The fan blades are 1.57mm thick aluminum riveted to a 3.9mm thick steel spider that attaches to a 15.9mm diameter shaft. This particular model of blade has exhibited early fatigue failure in the field, so its modes and dynamic performance are being assessed to better understand the failure. It is ideal to test the fan with a non-contact transducer and exciter in order to avoid the perturbing small blade-to-blade variations that might have an important effect on its performance.

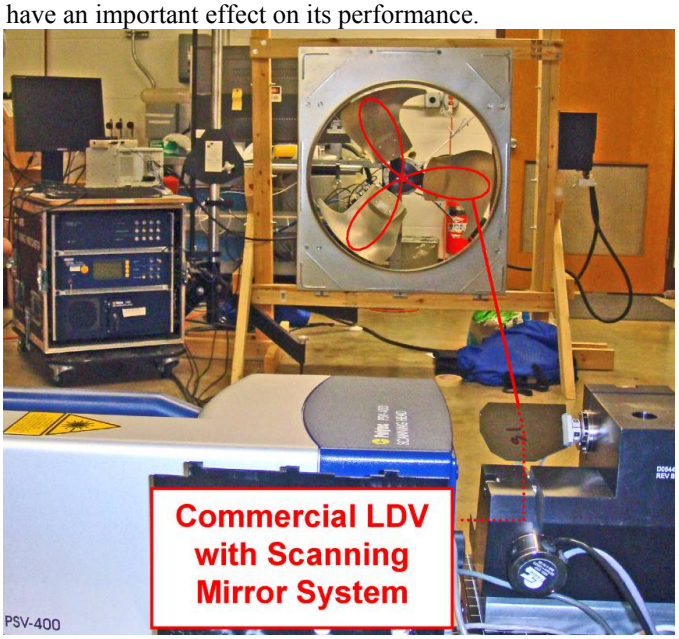

FIGURE 1. Photograph of experimental setup used to test a rotating fan with CSLDV

The results presented in this work were obtained using a cloverleaf scan pattern, constructed by sweeping the laser such that the radial position of the laser is given by

$$r(t) = \cos(3\omega_p t - \gamma) \tag{5}$$

where ω_p is the frequency with which the pattern rotates and γ is chosen such that the pattern is aligned with the blades of the fan. This scan pattern is illustrated schematically in FIGURE 1. The radial position in Eq. (5) can be converted to a position in terms of the *x*- and *y*- positions of the laser spot, which are proportional to the mirror angles θ_x and θ_y.

$$\begin{aligned} x(t) &= r(t)\cos(\theta_p) \\ y(t) &= r(t)\sin(\theta_p) \end{aligned} \tag{6}$$

Since the angle of the scan pattern, θ_p, is simply $\theta_p = \omega_p t$, one finds that x(t) and y(t) are two-harmonic signals given by

$$\begin{aligned} x(t) &= \frac{1}{2}(\cos(2\omega_p t - \gamma) + \cos(4\omega_p t - \gamma)) \\ y(t) &= \frac{1}{2}(-\sin(2\omega_p t - \gamma) + \sin(4\omega_p t - \gamma)) \end{aligned} \tag{7}$$

Hence, the fundamental frequency of this scan pattern is $\omega_A = 2\omega_p$. The pattern can be made to track a rotating fan by adjusting the phase γ in real time using the signal from the shaft encoder.

It is important to note that this scan pattern falls off of the structure near the root of the blade. This was found to increase the noise level in the measurements, so it certainly was not ideal, but this pattern was used anyway since it is the simplest pattern that captures the global motion of the fan; time and resources did not permit implementing a more complicated pattern.

3.1. CSLDV results on parked fan

The CSLDV approach was first used to extract several modes from the parked fan using the cloverleaf pattern described previously. The fan was excited using an instrumented hammer at 30 points, and each time the LDV signal was recorded as the laser spot swept the fan. The mirror signals were also recorded and the frequency of the scan pattern, ω_A, was found by fitting a multi-sine to the measured mirror signals using least squares, since it is important to know that quantity precisely (e.g. to one part in about 1e5) in order to accurately resample the CSLDV measurement. In all of the following, the mirror voltages were used directly. These can be converted to the angular displacements of the mirrors using the formula θ = (Mirror Voltage) × (4°/V).

Once the frequency of the scan pattern was precisely known, the measurements were lifted, making each measurement a single-input-multi-output measurement, and the resulting collection of multi-input-multi-output measurements was processed with the AMI modal parameter identification algorithm [12,13] to find the natural frequencies, damping ratios and mode shapes of the structure. The identified natural frequencies were un-aliased as described in [7] and the residue vectors obtained by AMI were then post-processed to obtain the mode shapes as a function of position along the scan path. A subset of the identified modes are shown in TABLE 1 from measurements with cloverleaf patterns at two fundamental frequencies and with a 'figure8' pattern which will be described later.

TABLE 1 Experimental modes of the structure identified from cloverleaf and *figure8* CSLDV measurements on the parked condenser fan.

	Cloverleaf CSLDV				***figure8* CSLDV**		
	53 Hz		**55 Hz**		**100 Hz**		
Mode	**fn**	**Zeta**	**fn**	**Zeta**	**fn**	**Zeta**	**Shape**
1	20.90	0.0065	21.05	0.0042	21.19	0.0143	1B +/-/0
2	21.20	0.0043	21.24	0.0037	21.41	0.0026	1B +/0/-
3	23.94	0.0022	23.95	0.0020	23.73	0.0027	1B +/+/+
4	35.57	0.0017	35.58	0.0016	35.27	0.0025	1BTw +/-/0
5	35.67	0.0025	35.68	0.0024	35.81	0.0026	1BTw +/0/-
6	37.68	0.0014	37.68	0.0012	37.69	0.0014	1BTw +/+/+
7	122.91	0.0010	122.77	0.0027	-	-	
8	165.29	0.0005	-	-	165.12	0.0010	
9	186.01	0.0006	-	-	-	-	
10	199.33	0.0003	-	-	199.23	0.0008	

The measured mirror signal was averaged over all measured cycles, and the mode shapes were then plotted versus the average scan path. The first six modes are plotted in FIGURE 2 through FIGURE 4 and the tenth mode is shown in FIGURE 5. Recall that the mode shape is only measured along the scan path. The path was meshed as shown with black lines and the coloring on the surface was added by interpolating between measurement points (using Matlab's 'patch' function) to aid in visualizing the mode shapes

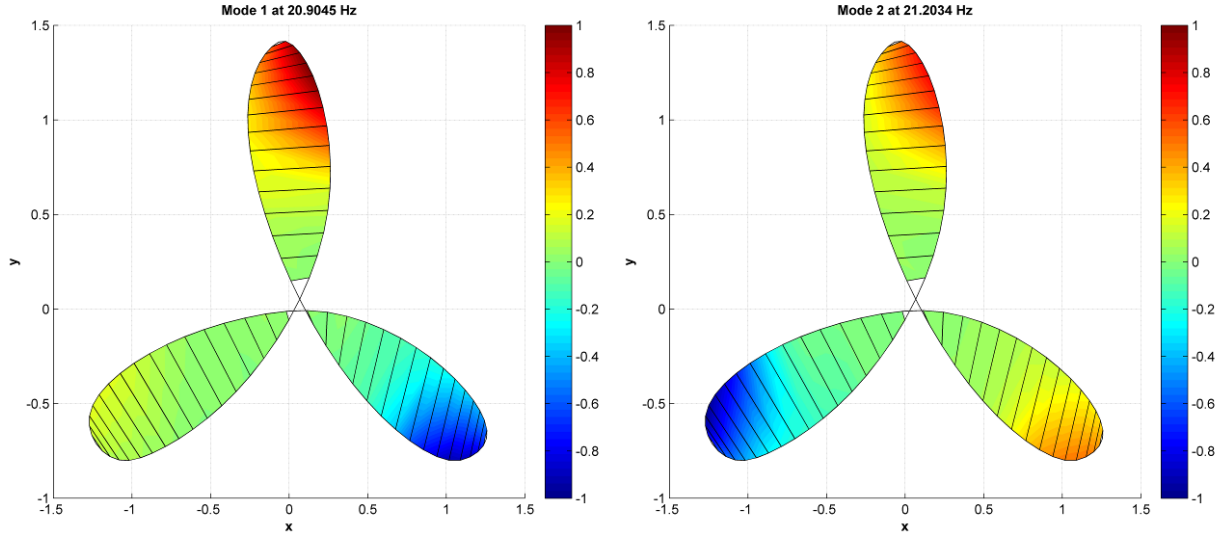

FIGURE 2. Mode shapes of the 1st (left) and 2nd (right) modes identified by CSLDV on the parked fan.

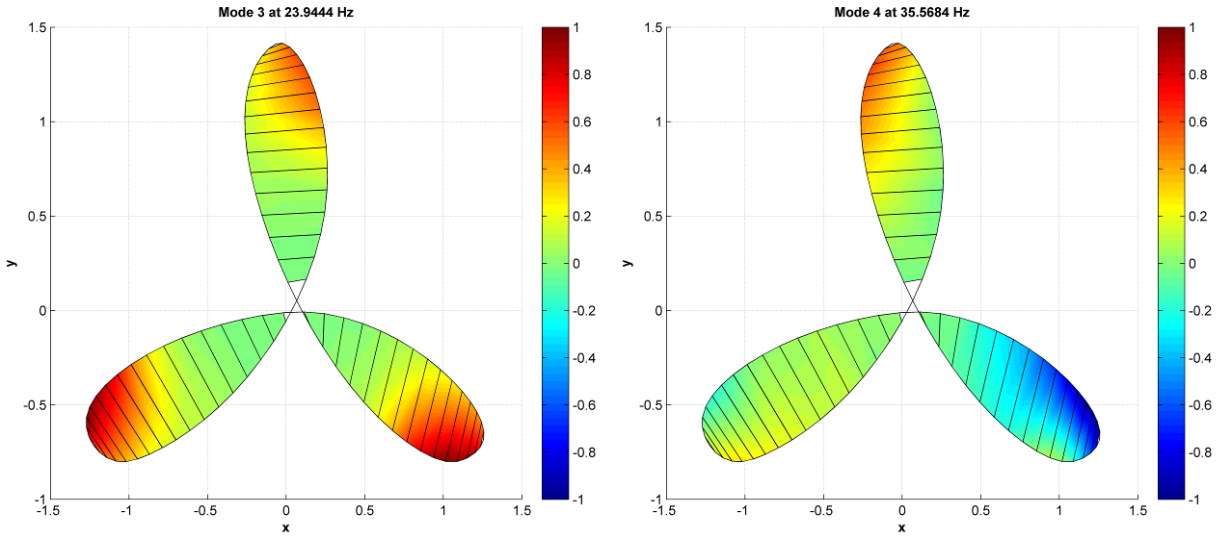

FIGURE 3. Mode shapes of the 3rd (left) and 4th (right) modes identified by CSLDV on the parked fan.

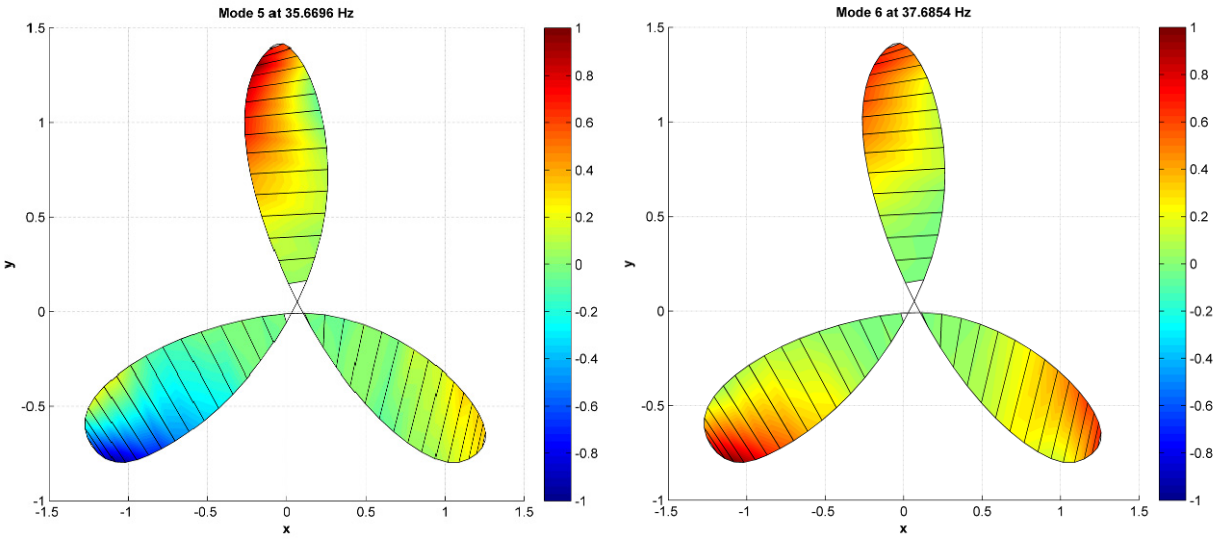

FIGURE 4. Mode shapes of the 5th (left) and 6th (right) modes identified by CSLDV on the parked fan.

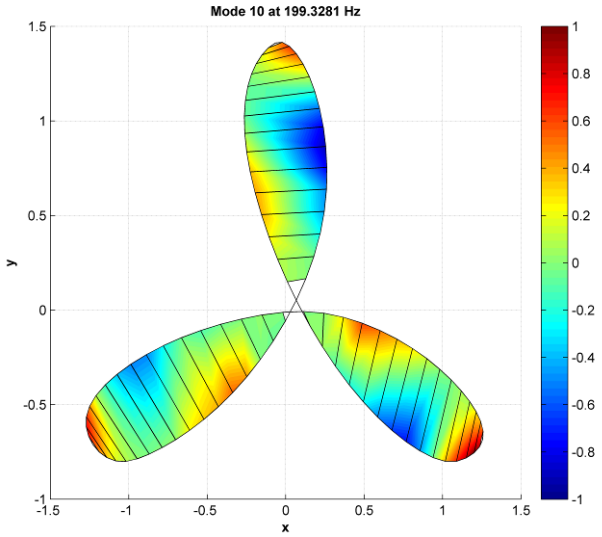

FIGURE 5. Mode shape of the 10th mode identified by CSLDV on the parked fan.

The natural frequencies of the fan agree with what one would expect theoretically. If the motor were sufficiently massive and the support structure and spider infinitely rigid, one would expect to obtain three repeated frequencies for each bending or torsion mode since each of the blades is nominally identical. The actual fan behaves somewhat differently due to weak coupling between the fan blades caused by the compliance of the spider and the compliance of the support structure. However, the modes still appear in groups of three all having similar natural frequencies. This is evidenced by the fact that the shape of the deformation of each of the individual blades is similar in modes 1-3; only the amplitude of each blade seems to change. The same is true for Modes 4-6. The highest frequency mode in each of the first three clusters is a symmetric mode in which all blades flap in unison. The other frequencies and their mode patterns are governed by the asymmetry of the supporting structure. For example, in the first mode the fan bends about a line parallel to the axis of the lower-left blade. This suggests that the supporting structure is most compliant about that axis. Mode 4 shows a similar pattern, supporting this observation. These features were summarized in TABLE 1 using the shape descriptors. In those columns, "1B" denotes the first bending mode of the blades, "1BTw" the first bend-twist mode of the blades, and "+/0/+" signifies that the first (top-blade in, e.g.

FIGURE 2-FIGURE 5) bends upward, the 2nd blade (proceeding clockwise) doesn't bend at all while the third blade (bottom) bends upwards as well.

The mode shapes acquired seem to be reasonably clean, considering that they were acquired from a relatively small number of measurements. Two scan frequencies were used in order to estimate the variance in the mode shapes due to the CSLDV approach. TABLE 2 assesses the consistency of the mode shapes, presenting the MAC between each of the shapes presented above (found with a 53 Hz scan frequency) and the corresponding shapes found with a 55 Hz scan frequency. The maximum difference is also presented, as a percentage of the largest deformation in each mode. That was computed by scaling each mode shape to the same maximum value, interpolating each shape onto a common set of instants within T_A, and then subtracting the shapes.

TABLE 2 Comparison of Mode Shapes Identified at 53 Hz and 55 Hz Scan Frequencies.

Mode	MAC	Max Difference (%)
1	0.977	12.56
2	0.9974	4.05
3	0.9944	8.91
4	0.9919	6.9
5	0.9815	16.76
6	0.9902	8.9
7	0.9532	30.43

One drawback of the cloverleaf scan pattern is the absence of measurement points interior to the scan path. Different scan patterns can be used to improve the measurement density in regions of interest. For example, a two-lobe *figure8* scan can be performed on a single blade of the fan by sweeping the laser with a single harmonic signal in the *x*- and *y*-directions, of frequency $2\omega_A$ and ω_A, respectively. The shape of this pattern results in measurements on the interior of a lobe on the cloverleaf scans in FIGURE 2-FIGURE 5. FIGURE 6 provides two views of the identified 2nd mode shape from measuring the top-blade of the fan with a 100 Hz *figure8* scan (ω_A = 100 Hz), and is plotted superposed with the results for mode 2 from FIGURE 2. The modes are scaled to have maximum amplitude of one.

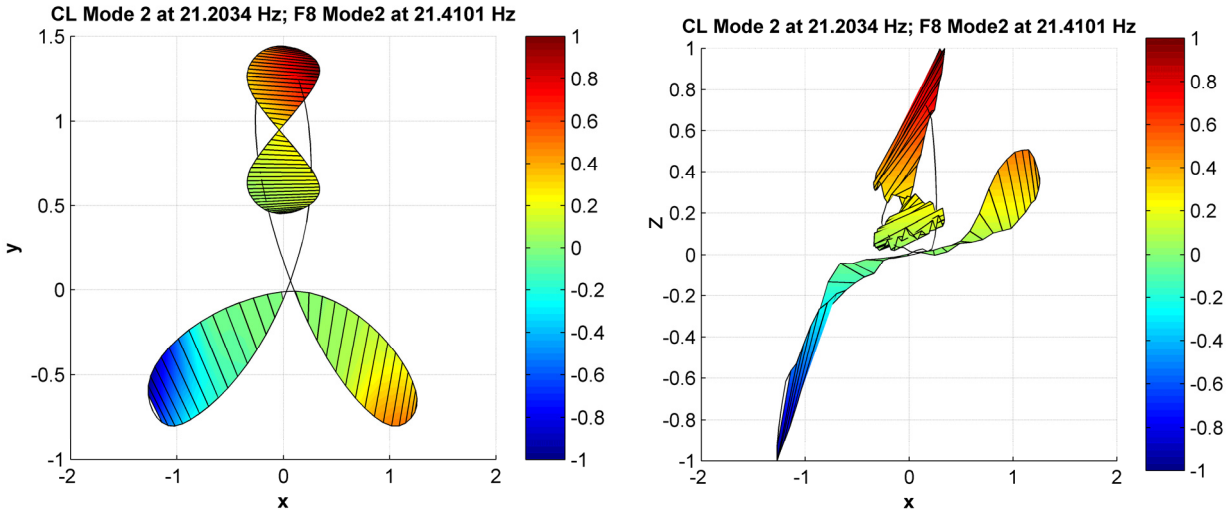

FIGURE 6. Two different 3D views of the shape of the 2nd mode identified by CSLDV on the parked fan from cloverleaf and *figure8* measurements. The colored surface on the top blade is omitted for clarity.

The mode shapes obtained from the *figure8* measurements agree quite well with the cloverleaf shapes, although some additional noise is present in this measurement, probably due to laser speckle caused by the high scan frequency of the mirrors. The increased resolution of the *figure*8 seems to reveal curvature near the tip that was not observed in the cloverleaf. One could use a variety of scan patterns such as this to maximize the proportion of the geometry that is interrogated.

3.2. Tracking-CSLDV on rotating fan

Once the baseline modal parameters of the fan had been established, measurements were acquired as the fan rotated. A variable frequency drive was used to drive the fan motor at constant speed, ranging from 3 to 10 Hz (180 to 600 RPM). The lower bound was the lowest speed at which the inverter was capable of driving the motor, while the upper was limited by the dynamics of the mirrors and the current supplied to the galvanometers. The fan was excited ten times at each speed using a small projectile. After the measurements were lifted, the spectra of some were visually very different from others, so they were discarded. It is important to note that the input was difficult to control. The same excitation method was also tested on the parked fan, revealing that the exciter favored the higher frequency (~80-300 Hz) modes of the fan. The first six modes were fairly difficult to excite with the projectiles used in here.

When the fan is rotating, the mirror position signals in Eq. (7) are modulated by the time-varying angle of the shaft, so a slightly different procedure had to be used to find the rotation frequency and the scan frequency. As with the parked data, the mirror position signal was fit to a multi-sine, only now the fundamental frequency of the multi-sine was the rotational frequency of the fan (rather than the fundamental frequency of the scan pattern). The mirror scan frequencies in *x*- and *y*- show up at integer multiples of the rotation frequency. Once the rotation frequency was precisely known, the mirror signals were de-rotated using a coordinate transformation similar to what was given in Eq.(6). The de-rotated mirror signals were plotted in order to verify that the signal processing was correct and also to obtain a measure of how consistent the scan pattern was. FIGURE 7 shows the de-rotated mirror signal from one of the measurements taken when the fan was rotating at 5.16 Hz. The orientation of the pattern is arbitrary. For this work, the starting point in the measurements was chosen such that the dominant harmonic in the mirror signal was a pure cosine. This produces a different orientation than what was shown in FIGURE 2 through FIGURE 5.

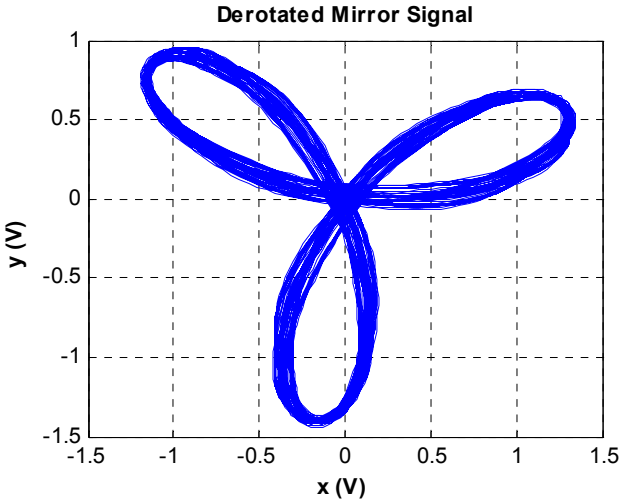

FIGURE 7. Measured mirror signals for 5.16Hz rotational speed, de-rotated and plotted *x* vs *y*. Some scatter is visible indicating that the scan pattern drifts slightly over the course of a measurement.

The mirror signal shown encompasses many cycles of the scan pattern, each of which is slightly different, leading to the scatter that is observed. The standard deviation of the x- and y- mirror signals was computed for each of the measurements, over all cycles of the scan frequency that were acquired (770 cycles for the 5.16Hz measurements). These were found to range between 0.032 to 0.046 Volts over the 10 measurements, or up to 3.5% of the measured signal. The variation was at least an order of magnitude smaller for the parked measurements described in Section 3.1.

Once the rotation frequency had been determined, the vibrometer signal was resampled such that it was synchronous with ω_A and only an integer number of cycles of the rotation were retained so that the FFT would contain lines at precisely the rotation frequency and its harmonics. This minimized the spreading of that frequency content to other spectral lines. The measurements were curve fit as described in the previous section, in order to determine the natural frequencies, mode shapes and damping ratios of the rotating fan. A composite or average of all of the lifted measurements for the fan is shown in FIGURE 8, for the 5.16Hz rotational speed. Sharp peaks are visible at the rotation frequency and its harmonics, the sharpest of which is 2-3 orders of magnitude larger than the

vibration peaks. This is to be expected since speckle noise resides at those frequencies and because the distance between the vibrometer and the measurement point changes as the fan rotates. Even then, four modal peaks were successfully fit by AMI. Two modes were detected at the 18 Hz peak, resulting in a total of five modes. These modes hardly stand out above the noise in the averaged measurement, but this was found to be somewhat of an artifact of the composite FRF. A composite of the response to a single input is shown in FIGURE 9, and there the modes can be seen to stand out more noticeably above the noise floor.

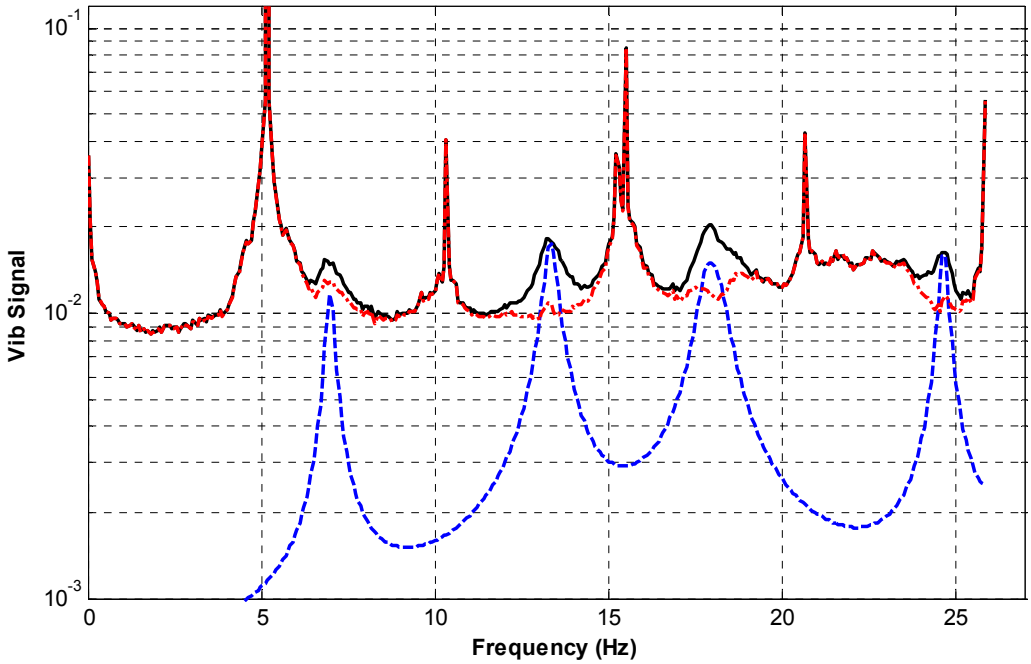

FIGURE 8. Composite of all 10 lifted TCSLDV measurements for 5.16 Hz rotational speed. (solid black) composite FRF of the lifted measurement, (dashed blue) composite of curve fit to the measurements (dash-dot red) composite of the difference between the measurement and the curve fit.

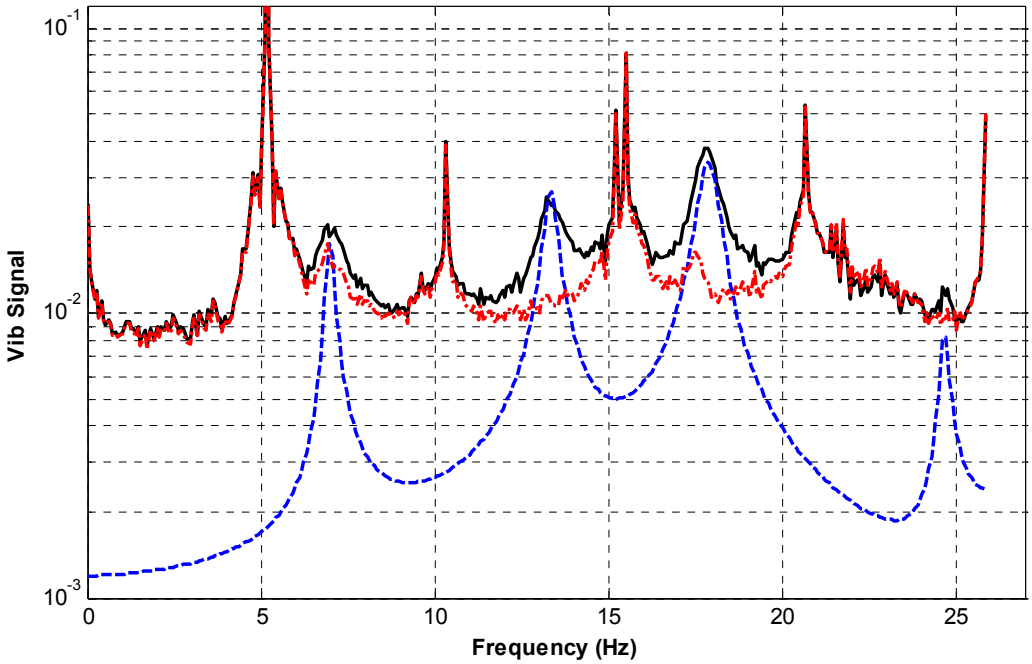

FIGURE 9. Composite of 9th lifted TCSLDV measurement for 5.16 Hz rotational speed. (solid black) composite FRF of the lifted measurement, (dashed blue) composite of curve fit to the measurements (dash-dot red) composite of the difference between the measurement and the curve fit.

At this juncture it is important to consider the choices available to the experimentalist that determine whether a particular mode is identified in the measurements. In practice one cannot choose the rotational speed of interest, yet one might be able to perturb it slightly to ensure that none of its harmonics coincide with a mode, since that would cause the mode to land in a contaminated frequency band in the lifted spectrum. One has more freedom in choosing the scan frequency; it could be any integer multiple of the rotational frequency. In the results shown in FIGURE 8 and FIGURE 9 the scan frequency was chosen to be ten times higher. The scan frequency determines how the modes alias in the lifted spectrum [7], so some choices might cause a mode of interest to overlap with one of the harmonics of the rotation frequency. Lower scan frequencies increase aliasing, while higher scan frequencies increases the demand on the mirror system and might cause the pattern to be less consistent over a measurement. One also must assure that two modes do not alias to the exact same frequency, otherwise their individual shapes will be difficult to distinguish. All of these considerations are easier to manage at higher rotational speeds where the harmonics of the rotation frequency are more widely spaced, but high speeds also place more significant demands on the mirror system. In this work, three rotational speeds were considered, 3.12 Hz, 4.8 Hz and 5.16 Hz. At 4.8 Hz one of the modes of the fan was excited by the 5th harmonic of the rotation frequency, and that was found to contaminate the results so those measurements were discarded.

TABLE 3 shows the natural frequencies identified from the measurements at 3.12 Hz and 5.16 Hz rotational speeds. Two frequencies are reported for each mode. The column labeled "fn ID" reports the aliased frequency at which the mode was actually identified (i.e. in FIGURE 8 or FIGURE 9). The column labeled "fn" shows the actual frequency of the mode, determined by un-aliasing the natural frequency identified by AMI. It is important to note that these frequencies were measured in the rotating frame of the fan, so one does not expect the natural frequencies to split into forward and backward whirling modes as one typically sees on Campbell diagrams for rotating machinery [14]. Shape descriptors are also provided, similar to what was given in TABLE 1, only here those refer first to the upper-left blade in FIGURE 10 - FIGURE 12.

TABLE 3 Natural Frequencies Identified by TCSLDV

Rot Freq	**Parked**	**3.1198 Hz (188 RPM)**			**5.1613 Hz (310 RPM)**		
Scan Freq	**53 Hz**	**49.917 Hz (16x)**			**51.613 Hz (10x)**		
Mode	**fn (Hz)**	**fn (Hz)**	**fn ID (Hz)**	**Shape**	**fn (Hz)**	**fn ID (Hz)**	**Shape**
3	23.94	24.18	24.18	1B +/+/+	24.63	24.63	1B +/+/+
4 (5)	35.57	35.86	14.06	1BTw +/-/0	-	-	-
6	37.69	37.91	12.01	1BTw +/+/+	38.29	13.33	1BTw +/+/+
7+	-	85.42	14.42	2B 0/+/+	85.07	18.16	2B +/0/+
7+	-	85.49	14.34	2B +/0.5/+	85.40	17.83	2B 0/+/+
7+	-	-	-	-	199.48	6.98	Plate

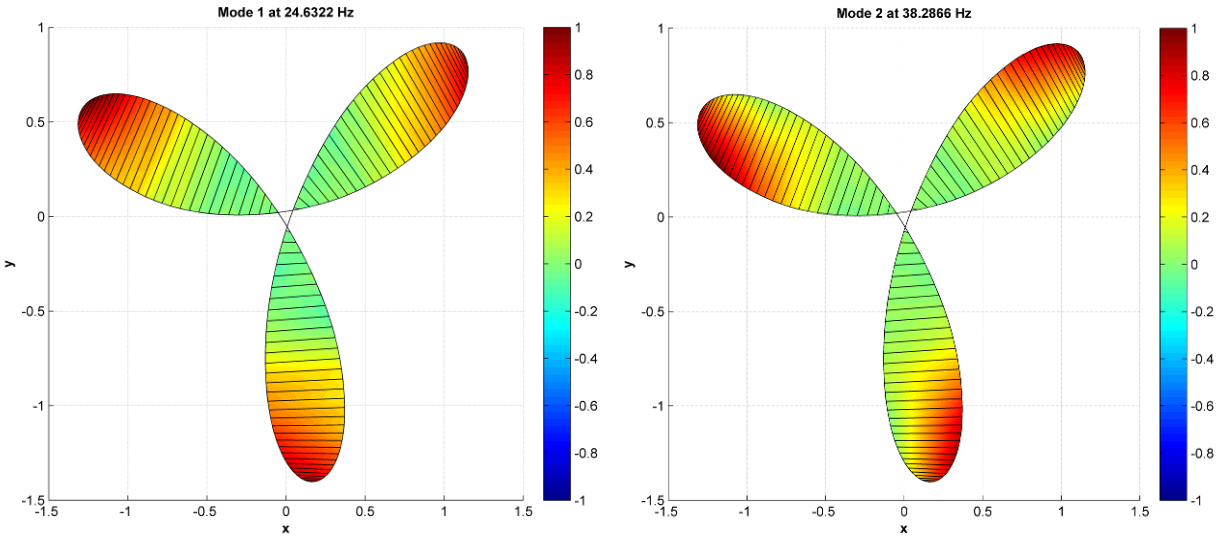

FIGURE 10. Mode shapes of the 1st (left) and 2nd (right) modes identified by tracking CSLDV at 5.16Hz rotational speed.

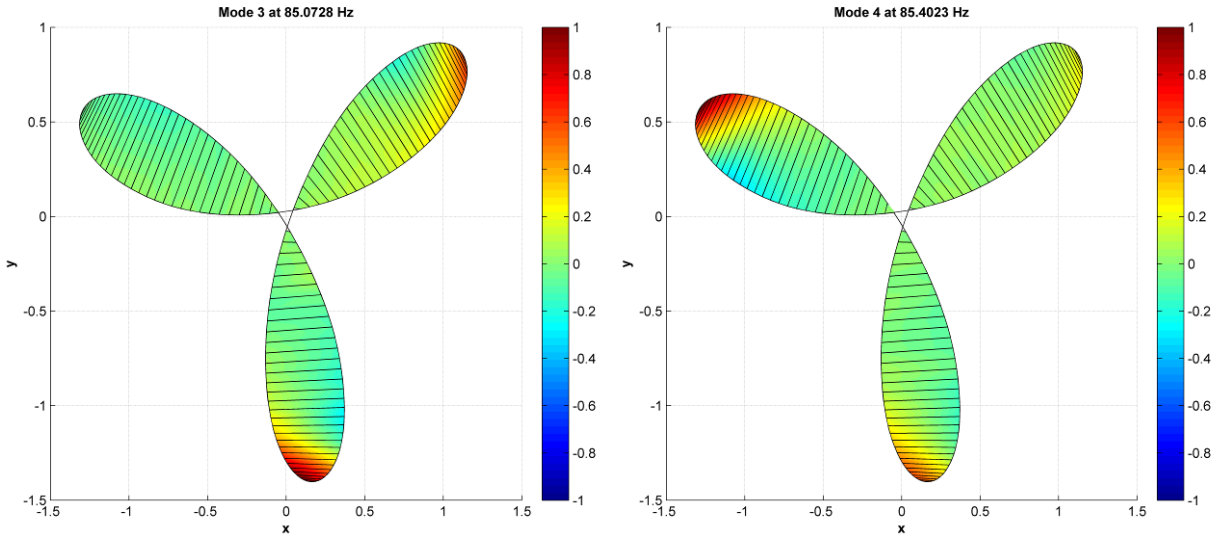

FIGURE 11. Mode shapes of the 3rd (left) and 4th (right) modes identified by tracking CSLDV at 5.16Hz rotational speed.

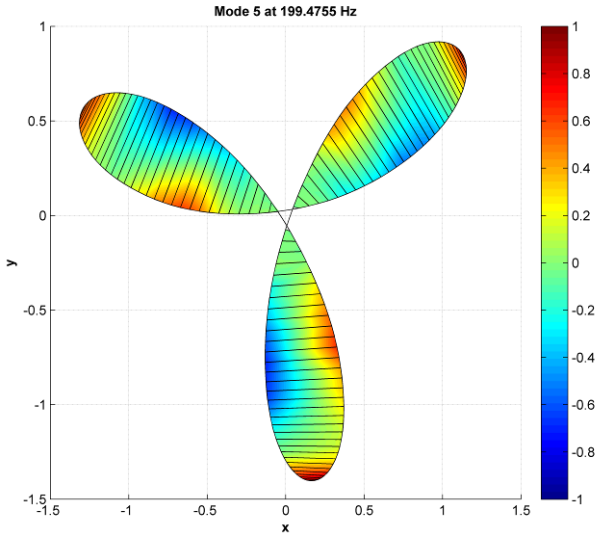

FIGURE 12. Mode shape of the 5th mode identified by tracking CSLDV at 5.16Hz rotational speed

Although only a few modes could be extracted, these results show pretty good consistency between the two rotational speeds. Some of the parked modes are also repeated in TABLE 3, and they also show good consistency. The frequency of the 3rd mode is 0.34 Hz higher at the 3.12 Hz rotational speed, and 0.45 Hz higher than that at 5.16 Hz, which seems to be a reasonable increase for centrifugal stiffening due to the increased speed. The 6th mode also increases, but only by 0.22 and 0.32 Hz. The 2nd bending modes of the blades (~85 Hz) do not show these trends, but those modes did overlap significantly in the frequency spectra, so one would not expect to be able to identify their individual frequencies very accurately. This might also explain why the shapes of these modes are not consistent between the two speeds. A finite element model of the fan was also constructed, but in spite of considerable effort it did not capture the natural frequencies of the fan very accurately. Only the fan and spider were modeled in detail, and it seemed to be difficult to adequately approximate the boundary condition provided by the motor/support. Even then, when that FEA model was evaluated at 3Hz and 5Hz rotational speeds it did show similar percentage shifts in the blade's natural frequencies, which seems to support the results presented here. It is also interesting that a 199 Hz mode was identified in the 5.16 Hz measurements. As noted previously, the projectile used to excite the system seemed to favor the higher frequency modes of the fan.

The mode shapes of the modes found at 5.16 Hz are shown in FIGURE 10 through FIGURE 12. In each case the shapes appear to be quite similar to those that were shown in FIGURE 2 through FIGURE 5. Future works will seek to compare these shapes in more detail and to quantify the differences and relate those to the centrifugal stiffening and aero-elastic effects.

4. CONCLUSIONS

This paper presented the development and the application of T-CSLDV, a tracking extension to Continuous Scan Laser Doppler Vibrometry (CSLDV) enabling one to measure the mode shapes at a large number of points quickly even as the structure rotates at significant speed during the measurement. The method was used to measure the modes of a parked fan, showing that repeatable results could be obtained over a scan pattern that encompassed all of the blades and at various scan frequencies. Measurements were also obtained from a rotating fan. Various mode shapes were extracted from the T-CSLDV measurements at two different rotational speeds and those were found to agree quite well with the modes obtained on the parked fan. The natural frequencies of each of the extracted modes also seemed to show reasonable trends with rotational speed, an encouraging result especially considering the difficulty in producing a reliable high-frequency scan pattern on the rotating structure.

The measurement quality seemed to be influenced to a significant extent by strong harmonics at the rotation frequency and its multiples. The effect of these harmonics was minimized by resampling the measurements to compress them as nearly as possible to single lines in the FFT. Even then, at these low rotational speeds only a small portion of the frequency band remained trustworthy. However, several accurate modes were extracted, and if the process were repeated at several rotational speeds then one would expect to be able to extract all of the modes of the fan. The CSLDV approach used here was only valid for the free response of a structure, so the blades were excited impulsively a few times for each measurement. The excitation level had to be relatively high so that the transient response dominated the response, which was difficult since the fan was fairly heavily damped. In some applications there are compelling reasons to use impulsive excitation, but for the system studied here it might have been preferable to instead utilize the excitation provided by the rotation of the fan itself. Future works should explore this possibility, perhaps using the output-only identification method presented in [15].

5. REFERENCES

1. P. Sriram, J. I. Craig, and S. Hanagud, "Scanning laser Doppler vibrometer for modal testing," International Journal of Analytical and Experimental Modal Analysis, vol. 5, pp. 155-167, 1990.
2. M. Martarelli, "Exploiting the Laser Scanning Facility for Vibration Measurements," Ph.D. Thesis, Imperial College of Science, Technology & Medicine, London: Imperial College, 2001.
3. P. Castellini, "Sviluppo e verifica sperimentale di una tecnica per la misura di vibrazione di oggetti rotanti (Development and experimental verification of a technique for measuring the vibration of rotating objects.)," Thesis: Università degli Studi di Padova, 1997.
4. P. Castellini and N. Paone, "Development of the tracking laser vibrometer: Performance and uncertainty analysis," Review of Scientific Instruments, vol. 71, pp. 4639-4647, 2000.
5. P. Castellini and E. P. Tomasini, "Image-based tracking laser Doppler vibrometer," Review of Scientific Instruments, vol. 75, pp. 222-32, 2004.
6. D. Di Maio and D. J. Ewins, "Use of Tracking-Continuous Scanning LDV (T-CSLDV) methods for vibration study of bladed disk assembly under operating conditions." vol. 1 Exeter, United kingdom: Chandos Publishing, 2008, pp. 317-330.
7. M. S. Allen and M. W. Sracic, "A New Method for Processing Impact Excited Continuous-Scan Laser Doppler Vibrometer Measurements," Mechanical Systems and Signal Processing, vol. 24, pp. 721–735, Available Online Nov. 2009 2010.
8. M. S. Allen and M. W. Sracic, "A Method for Generating Pseudo Single-Point FRFs from Continuous Scan Laser Vibrometer Measurements," in 26th International Modal Analysis Conference (IMAC XXVI) Orlando, Florida, 2008.
9. R. Ribichini, D. Di Maio, A. B. Stanbridge, and D. J. Ewins, "Impact Testing With a Continuously-Scanning LDV," in 26th International Modal Analysis Conference (IMAC XXVI) Orlando, Florida, 2008.
10. A. B. Stanbridge, M. Martarelli, and D. J. Ewins, "Scanning laser Doppler vibrometer applied to impact modal testing," in 17th International Modal Analysis Conference - IMAC XVII. vol. 1 Kissimmee, FL, USA: SEM, Bethel, CT, USA, 1999, pp. 986-991.
11. M. S. Allen, "Frequency-Domain Identification of Linear Time-Periodic Systems using LTI Techniques," Journal of Computational and Nonlinear Dynamics vol. 4, 24 Aug. 2009.
12. M. S. Allen and J. H. Ginsberg, "A Global, Single-Input-Multi-Output (SIMO) Implementation of the Algorithm of Mode Isolation and Applications to Analytical and Experimental Data," Mechanical Systems and Signal Processing, vol. 20, pp. 1090–1111, 2006.

13. M. S. Allen and J. H. Ginsberg, "Global, Hybrid, MIMO Implementation of the Algorithm of Mode Isolation," in 23rd International Modal Analysis Conference (IMAC XXIII) Orlando, Florida, 2005.
14. J. S. Rao, Rotor Dynamics, Third Edition ed. Daryaganj, New Delhi: New Age International, 1996.
15. M. S. Allen, M. W. Sracic, S. Chauhan, and M. H. Hansen, "Output-Only Modal Analysis of Linear Time Periodic Systems with Application to Wind Turbine Simulation Data," in 28th International Modal Analysis Conference (IMAC XXVIII) Jacksonville, Florida, 2010.